

Functionalized Supramolecular Nanoporous Arrays for Surface Templating

Luís M. A. Perdigão,^[a] Alex Saywell,^[a] Giselle N. Fontes,^[a, b] Paul A. Staniec,^[a] Gudrun Goretzki,^[c] Anna G. Phillips,^[c] Neil R. Champness,^{*,[c]} and Peter H. Beton^{*,[a]}

Abstract: Controlled self-assembly and chemical tailoring of bimolecular networks on surfaces is demonstrated using structural derivatives of 3,4:9,10-perylenetetracarboxylic diimide (PTCDI) combined with melamine (1,3,5-triazine-2,4,6-triamine). Two functionalised PTCDI derivatives have been synthesised, Br₂-PTCDI and di(propylthio)-PTCDI, through attachment of chemical side groups to the perylene core. Self-assembled struc-

tures formed by these molecules on a Ag-Si(111) $\sqrt{3}\times\sqrt{3}R30^\circ$ surface were studied with a room-temperature scanning tunneling microscope under ultra-high vacuum conditions. It is shown that the introduction of side groups can

have a significant effect upon both the structures formed, notably in the case of di(propylthio)-PTCDI which forms a previously unreported unimolecular hexagonal arrangement, and their entrapment behaviour. These results demonstrate a new route of functionalisation for network pores, opening up the possibility of designing nanostructured surface structures with chemical selectivity and applications in nanostructure templating.

Keywords: hydrogen bonds • melamine • perylenetetracarboxylic diimides • scanning probe microscopy • self-assembly

Introduction

The bottom-up approach to nanostructure fabrication offers new routes to the systematic preparation of nanostructures by design. One particularly promising approach is to utilise the principles and techniques embodied in the field of supramolecular chemistry.^[1,2] In particular, the use of supramolecular chemistry has demonstrated that a high degree of control can be exerted over molecular orientation by the use of non-covalent intermolecular interactions.^[3] Supra-

molecular chemistry offers not only the possibility to control self-assembly processes, but also, through chemical functionalisation of the constituent species, the potential for molecular recognition by the self-assembled architecture.^[4] Thus, the utilisation of supramolecular chemistry offers a highly flexible methodology for control of nanoscale structure.

Two-dimensional self-assembly of molecules on surfaces, when combined with scanning probe techniques, provides direct evidence of the great potential of this approach. In particular, self-assembled structures that are stabilised by intermolecular interactions such as hydrogen bonding, metal coordination and dipolar coupling have been demonstrated by using a variety of molecule-substrate systems.^[5-23] Furthermore, we have recently demonstrated the formation of two-dimensional bimolecular cavities stabilised by hydrogen bonding that may be used to trap diffusing species^[15-17] as guest molecules. In related work Stepanow et al.^[20] have demonstrated that the host-guest interaction may be modified through the inclusion of additional chemical groups within the framework molecules. Here we explore the possibility of adding host-guest selectivity to these pores through the rational design of the constituent molecules that form the network. We demonstrate that chemical functionality be introduced to such systems and also that functionalisation of the nanoscale architectures can lead to new self-assembled structures and the resultant host-guest properties of the nanoarchitecture can be tuned.

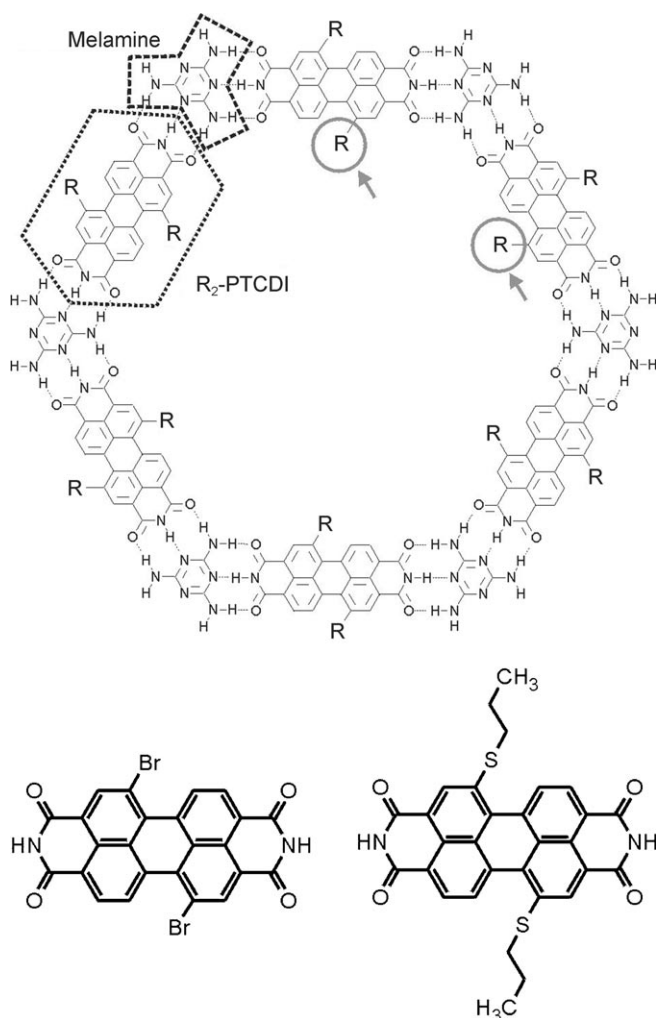
[a] Dr. L. M. A. Perdigão, A. Saywell, Dr. G. N. Fontes, Dr. P. A. Staniec, Prof. P. H. Beton
School of Physics and Astronomy
University of Nottingham, University Park
Nottingham NG7 2RD (UK)
Fax: (+44) 115-951-5180
E-mail: Peter.Beton@nottingham.ac.uk

[b] Dr. G. N. Fontes
Departamento de Física, ICEx
Universidade Federal de Minas Gerais, Ave. Antonio Carlos
6627-Belo Horizonte, CEP 30123-970 (Brazil)

[c] Dr. G. Goretzki, A. G. Phillips, Prof. N. R. Champness
School of Chemistry, University of Nottingham
University Park, Nottingham NG7 2RD (UK)
Fax: (+44) 115-951-3563
E-mail: Neil.Champness@nottingham.ac.uk

Supporting information for this article is available on the WWW under <http://dx.doi.org/10.1002/chem.200800476>.

Specifically we show that bimolecular honeycomb arrays can also be formed if the 3,4:9,10-perylenetetracarboxylic diimide (PTCDI) from the known hexagonal PTCDI/melamine arrangement^[15,16] (melamine = 1,3,5-triazine-2,4,6-triamine) is replaced with similar molecules that are functionalised through the attachment of a side group to the perylene core, generically called here R_2 -PTCDI (Scheme 1, top). The synthesis of perylene diimide derivatives has been extensively examined allowing the development of such molecules for a wide variety of applications;^[24] however, only a few examples of derivatised perylene diimides that maintain the non-alkylated imide group have been previously described.^[25] The diimide termination, present in the original PTCDI molecule and which is essential for the formation of the triple hydrogen bond with melamine and responsible for the stabilisation of the hexagonal arrangement observed in the mixtures, is preserved in our structural design.

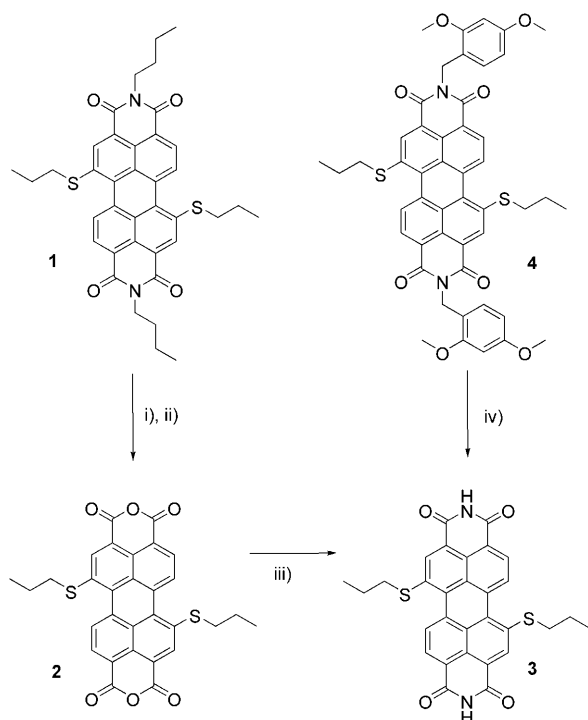


Scheme 1. Top: Target hexagonal arrangement with R_2 -PTCDI and melamine stabilised by a triple hydrogen bond. The functionalisation of the cavities is achieved through the attachment of chemical groups (represented with R and highlighted with grey circles) onto the sides of the perylene core of the PTCDI molecule. Bottom left and right: Br_2 -PTCDI and di(propylthio)-PTCDI, respectively.

This type of system combines the templating effect that has been demonstrated previously for such hexagonal nanoarchitectures with the possibility of molecular recognition driven by the functional group added to the original PTCDI molecule. We have studied two variants of R_2 -PTCDI, firstly with R being bromine, (Scheme 1, bottom left), and the other with propylthio substituents (Scheme 1, bottom right). Although each of these molecules forms characteristic assemblies on the $Ag-Si(111)\sqrt{3}\times\sqrt{3}R30^\circ$ surface, they differ from the arrangements of the parent compound PTCDI on the same surface. Whereas Br_2 -PTCDI forms a nanoporous hexagonal arrangement by co-self-assembly with melamine, di(propylthio)-PTCDI forms a unimolecular self-assembled nanoporous hexagonal arrangement, the periodicity of which can be increased by the introduction of melamine and subsequent bimolecular structure self-assembly.

Results and Discussion

Chemical synthesis: Br_2 -PTCDI was prepared by bromination of the 3,4:9,10-perylenetetracarboxylic dianhydride (PTCDA) to afford a mixture of isomers Br_2 -PTCDA.^[26] The preparation of Br_2 -PTCDA yields a mixture of both 1,7- and 1,6-isomers in an estimated 4:1 ratio that it has not proven possible to separate.^[26b] Subsequent reaction of Br_2 -PTCDA with $NH_4OH_{(aq)}$ affords Br_2 -PTCDI as a highly insoluble red solid. Perylene diimide species, without alkyl/aryl tail groups, are notoriously insoluble in common organic solvents and thus separation of the 1,6- and 1,7-isomers is not feasible at this stage of the synthetic procedure. Di(propylthio)-PTCDI was prepared by two alternative routes (Scheme 2). Introduction of the propanethio appendages is successfully achieved by the reaction of propanethiol with either N,N' -di(*n*-butyl)-1,7-dibromoperylene-3,4:9,10-tetracarboxylic acid diimide or N,N' -di(2,4-dimethoxy)-benzyl)-1,7-dibromoperylene-3,4:9,10-tetracarboxylic acid diimide in the presence of a base to give compound **1** or **4**, respectively. Compound **1** can be converted to the corresponding disubstituted dithioether-PTCDI by using the traditional methodology^[26b] of converting the dialkyl perylene diimide to the corresponding dianhydride **2** followed by subsequent conversion to diimide **3**. This synthetic procedure successfully produces the desired product, but in a yield of only 45% from **1** and is a relatively aggressive synthetic strategy, using a 100-fold excess of KOH as a reagent. Thus, we have established a new procedure for the synthesis of PTCDI molecules derivatised in the so-called bay region. By using 2,4-dimethoxybenzyl alkylated intermediates (e.g., **4**) in the synthetic strategy we are able to convert the 2,4-dimethoxybenzyl-protected perylene species to the desired PTCDI product by a simple deprotection step, using methanesulfonic acid, without the need to prepare an intermediary anhydride species. This mild approach, in comparison to the conventional procedure, affords the desired species **3** in 89% from the dialkylated species **4**. A similar approach of protection/deprotection for the formation of diimide PTCDI deriva-



Scheme 2. Reaction scheme illustrating synthetic strategy to PTDCI-derivatives: i) KOH, *i*PrOH; ii) CH₃COOH, 95%; iii) NH₄OH, 47%; iv) MeSO₃H, C₆H₅Me, 89%.

tives has recently been reported by Würthner et al. using the cleavage of *N*-methylbenzyl derivatised PTCDI-based species using BBr₃.^[25a] Unfortunately we were unable to separate the 1,6- and 1,7-isomers of either **1** or **4**, although the 1,7-isomer is the major component with trace amounts of the 1,6-isomer present in either material and thus the final product **3** is predominantly the 1,7-isomer with only traces of the 1,6-isomer present.

Surface studies

Br₂-PTCDI: Following deposition of Br₂-PTCDI onto the Ag-Si surface, one-dimensional molecular rows are formed as shown in the STM images in Figure 1a. A higher resolution STM image is shown in Figure 1b in which the Ag-Si reconstruction is visible with darker contrast regions corresponding to a silicon trimer.^[27] In common with PTCDA and PTCDI^[16,28] on this surface, the Br₂-PTCDI molecules have intramolecular contrast corresponding to a double lobe that runs parallel to the long axis of the molecules. From this identification it is possible to determine the molecular position and orientation relative to the substrate. The self-assembled rows adopt an orientation parallel to the $\langle 11\bar{2} \rangle$ direction of the substrate with a measured molecule-molecule spacing within a row of (14.8 ± 0.2) Å. Individual molecules within a row can be resolved, see white dashed rectangle in Figure 1b, and from these high-resolution images we propose a model for a row with a width corresponding to a single molecule. This is shown in Figure 1c, which is stabi-

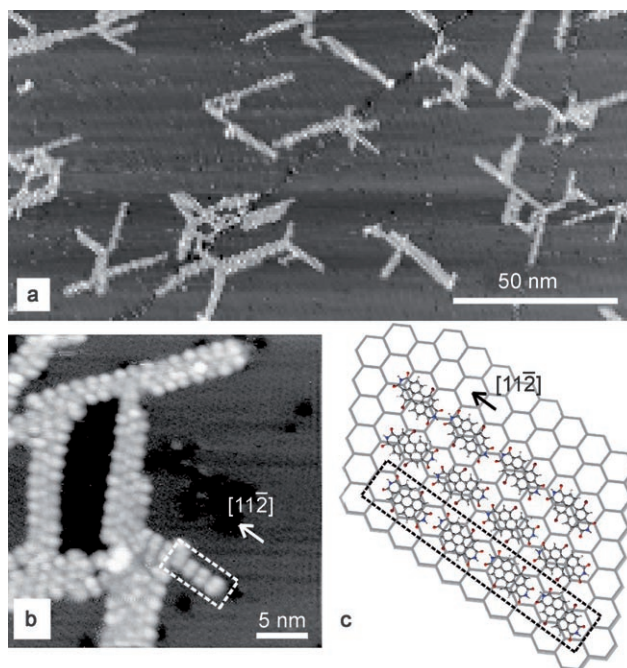


Figure 1. a) STM image of the Ag-Si(111) $\sqrt{3} \times \sqrt{3}R30^\circ$ surface, after Br₂-PTCDI sublimation ($V_{\text{sample}} = -2$ V, $I_{\text{tunnel}} = 0.05$ nA), in which the formation of elongated rows following well-defined directions is evident. b) Higher resolution image of an area with different Br₂-PTCDI row widths ($V_{\text{sample}} = -2$ V, $I_{\text{tunnel}} = 0.05$ nA). A single molecular row is highlighted with a white dashed rectangle. c) Schematic model for the single molecular row highlighted (substrate reconstruction is represented with the hexagonal grid, with the centres corresponding to silicon trimers) in b), with each molecule forming a double hydrogen bond with neighbouring molecules and the row parallel to the substrate $\langle 11\bar{2} \rangle$ direction. The dimension of each STM image is given in the inserted scale bar.

lised by a double hydrogen bond between neighbouring molecules, linked through the imide terminations.^[28-31]

The arrangement proposed for single Br₂-PTCDI chains is similar to that observed for single rows of PTCDI on the same substrate.^[28] However, for PTCDI the rows are much shorter and co-exist with large two-dimensional islands. For Br₂-PTCDI many of the molecular rows have widths corresponding to one or two molecules, but we do not observe extended two-dimensional islands (for an analysis of the distribution of row widths see the Supporting Information). Thus the addition of the -Br appendage to the PTCDI has resulted in an enhanced stability of one-dimensional rows relative to extended islands. In recent numerical studies of anisotropic growth^[32,33] it has been demonstrated that such an enhancement can result either from an increase in the hydrogen-bonding interaction or a reduction in the intermolecular interactions that stabilise row-row coupling in island formation. In the case studied here the addition of the -Br appendage has a negligible effect of the strength of hydrogen bonding. However, the presence of this electronegative species on the perylene core is expected to give rise to a repulsive Br-Br intermolecular interactions that leads to a reduction in inter-row interactions. This results in a relative

destabilisation of two-dimensional growth in favour of row formation.

The deposition of melamine onto a sub-monolayer of Br₂-PTCDI coverage, followed by annealing at $\approx 60^\circ\text{C}$, results in the formation of a bimolecular honeycomb arrangement as shown in the STM image in Figure 2a. A magnified image of the network with detail of the surface reconstruction is shown in Figure 2b. The periodicity of the network is $\approx 35 \text{ \AA}$, and the network lattice vectors are parallel to the substrate $\langle 1\bar{1}0 \rangle$ direction. These dimensions are identical, within experimental error, to those previously reported for a PTCDI/melamine network.^[16] This shows clearly that the observed arrangement is a direct analogue to the previously reported network in which Br₂-PTCDI molecules adopt the hexagonal structure illustrated in Scheme 1, top (see superimposed molecular model in Figure 2b).

One difference with our previous work is that we observe a complete conversion of the Br₂-PTCDI into the hexagonal framework. For unfunctionalised PTCDI we observe a coexistence between the bimolecular hexagonal framework and two-dimensional PTCDI islands. The complete conversion of the brominated derivative, accounted for by the destabilisation of two-dimensional Br₂-PTCDI islands, is potentially significant for the formation of large-area, single-phase networks and offers the possibility of much greater homogeneity of entrapment properties. Furthermore this difference confirms that the properties of supramolecular arrays may be engineered through relatively minor changes in the constituent molecules. Although the bimolecular Br₂-PTCDI/melamine honeycomb network can in principle exhibit chirality (see Figure 2b) we were unable to determine the precise positioning of individual bromine substituents and therefore are unable to establish the precise extent of chirality exhibited by the honeycomb framework.

Most importantly these results confirm the hypothesis that the formation of bimolecular hexagonal assemblies between R₂-PTCDI and melamine is possible. The use of Br₂-PTCDI provides the first demonstration of a route to functionalise the cavities of the PTCDI/melamine regular hexagonal arrangement. It is worth noting that Br₂-PTCDI is a synthetic precursor to a range of R₂-PTCDI molecules^[25] and as such the Br₂-PTCDI/melamine array offers the potential for further chemical functionalisation.

The C₆₀-entrapment properties of this network were compared with previous results on PTCDI/melamine assemblies.^[15,16] The STM images (Figure 2c) show the formation of C₆₀ heptamers within the pores as observed when C₆₀ is deposited on the PTCDI/melamine porous network. This indicates that both Br₂-PTCDI/melamine and PTCDI/melamine networks stabilise C₆₀ clusters with similar geometries, most likely as a result of the relatively short steric bulk of the Br appendages. Interestingly we have observed that the heptamers captured in the brominated cavities, as compared with the parent PTCDI/melamine array, are more susceptible to interactions with the tip of the scanning probe microscope providing indirect evidence that they are less strongly bound.

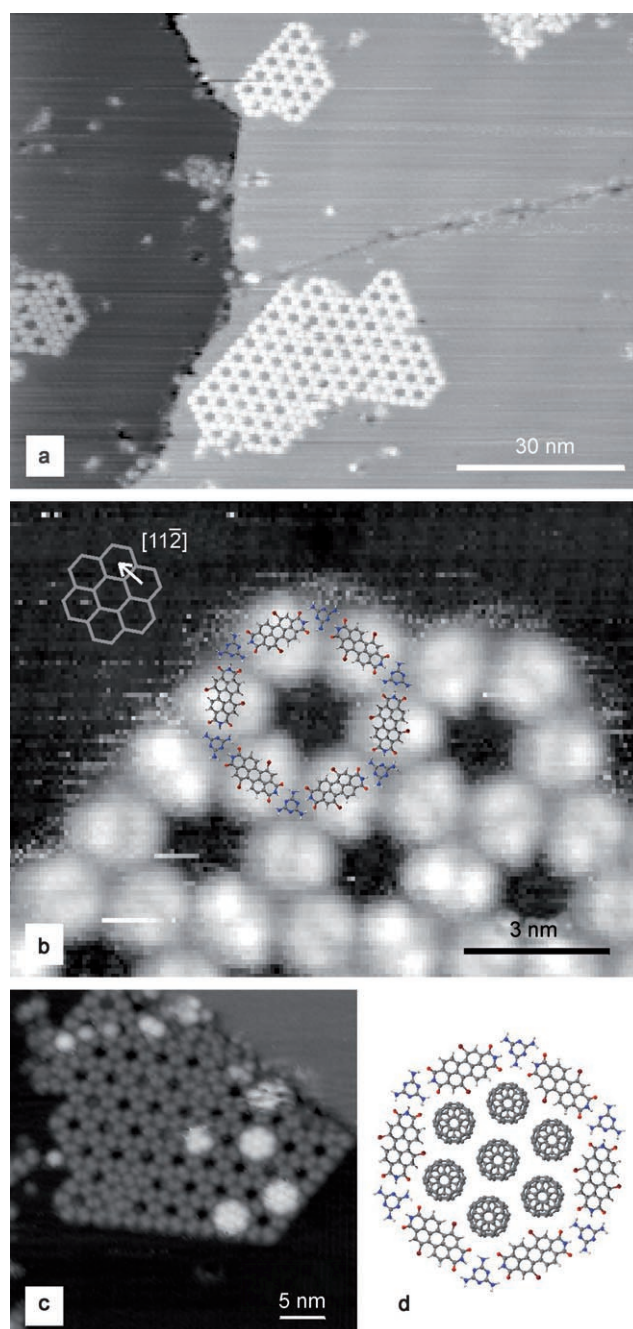


Figure 2. a) Image showing hexagonal supermolecular structures formed with Br₂-PTCDI and melamine on the Ag-Si(111) $\sqrt{3} \times \sqrt{3}R30^\circ$ surface ($V_{\text{sample}} = +2.1 \text{ V}$, $I_{\text{tunnel}} = 0.05 \text{ nA}$). b) Higher resolution image ($V_{\text{sample}} = -2 \text{ V}$, $I_{\text{tunnel}} = 0.05 \text{ nA}$) of the Br₂-PTCDI/melamine hexagonal network, in which the double protrusion of each Br₂-PTCDI molecule is apparent. The hexagonal mesh represents the surface reconstruction with the hexagon centres corresponding to silicon trimers (see text). One of the $\langle 1\bar{1}2 \rangle$ surface directions is represented with the white arrow. A molecular model is superimposed for clarification. c) Image ($V_{\text{sample}} = -2.8 \text{ V}$, $I_{\text{tunnel}} = 0.03 \text{ nA}$) showing three captured C₆₀ heptamers within the cavities of the Br₂-PTCDI/melamine network. d) Molecular model of a C₆₀ heptamer inside a Br₂-PTCDI/melamine pore. The dimension of each STM image is given in the inserted scale bar.

Di(propylthio)-PTCDI: Deposition of 0.4 monolayers of di(propylthio)-PTCDI onto a clean Ag-Si surface results in

the formation of two-dimensional self-assembled structures, in contrast to Br₂-PTCDI. The STM image shown in Figure 3a reveals two co-existing domains labelled as α and β . Whereas in the β region the molecules form a close-packed array, those in the α region adopt a very interesting hexagonal arrangement (shown in more detail in Figure 3b; see Supporting Information for discussion of region β). The hexagonal structure has a periodicity of 28.3 ± 1 Å, and an angle of $16 \pm 2^\circ$ relative to the $\langle 11\bar{2} \rangle$ substrate direction. The measured periodicity is significantly smaller than the dimensions observed for the PTCDI/melamine complex (Scheme 1, top),^[15,16] and, moreover, cannot arise from an arrangement in which the molecules are linked by double hydrogen bonds, as observed for Br₂-PTCDI.

We propose a model, shown in Figure 3c in which each vertex is formed by a junction of three molecules and stabilised by three hydrogen bonds between the N–H groups on one molecule and one of the C=O groups on a neighbouring molecule. This triple vertex bonding configuration is similar to the stabilising linkage proposed for cyanuric acid on the same surface^[34] and is chiral.

It is clear that PTCDI, even in the absence of the side groups, could adopt this hexagonal configuration for which the overall number of hydrogen bonds per molecule is the same as in the rows formed by Br₂-PTCDI and PTCDI. However, the hexagonal arrangement is only observed for molecules that incorporate the propylthio side groups. We hypothesise that an additional attractive C–H...O hydrogen-bonding interaction may exist between the propylthio chains and the oxygen atom on a neighbouring molecule that is not bound to an imide group within the trigonal vertex. The stabilisation energy obtained for the vertex in this configuration, calculated from density functional theory (see Supporting Information) is 0.86 eV. For an alternative configuration, in which the vertex chirality is preserved but the propylthio chains are attached to the other bay-region carbon atoms (see arrows in Figure 3c and Supporting Information), a stabilisation energy of 0.70 eV was calculated. Thus, the configuration shown in Figure 3c, with the propylthio chains closer to the available oxygen atom, is calculated to be more stable. The stabilisation energy calculated for a vertex composed with three PTCDI molecules (with no side chains) is 0.78 eV, lower than the energy obtained for the suggested vertex, further demonstrating the contribution of the side chains in stabilising the structure.

The additional stabilisation provided by the side chains implies that they must adopt a specific conformation. Note that, due to their flexibility arising from the potential for rotation about the C–C bond axes, there are several different conformations which the molecular side chains might adopt. In this context the stabilisation may be considered as an adaptive effect in which the molecule adopts a specific conformation in response to its local environment. The link between flexibility of molecules and their potential for interlocking through adopting mutually energetically favourable conformations has recently been highlighted for adsorbed amino acids.^[35]

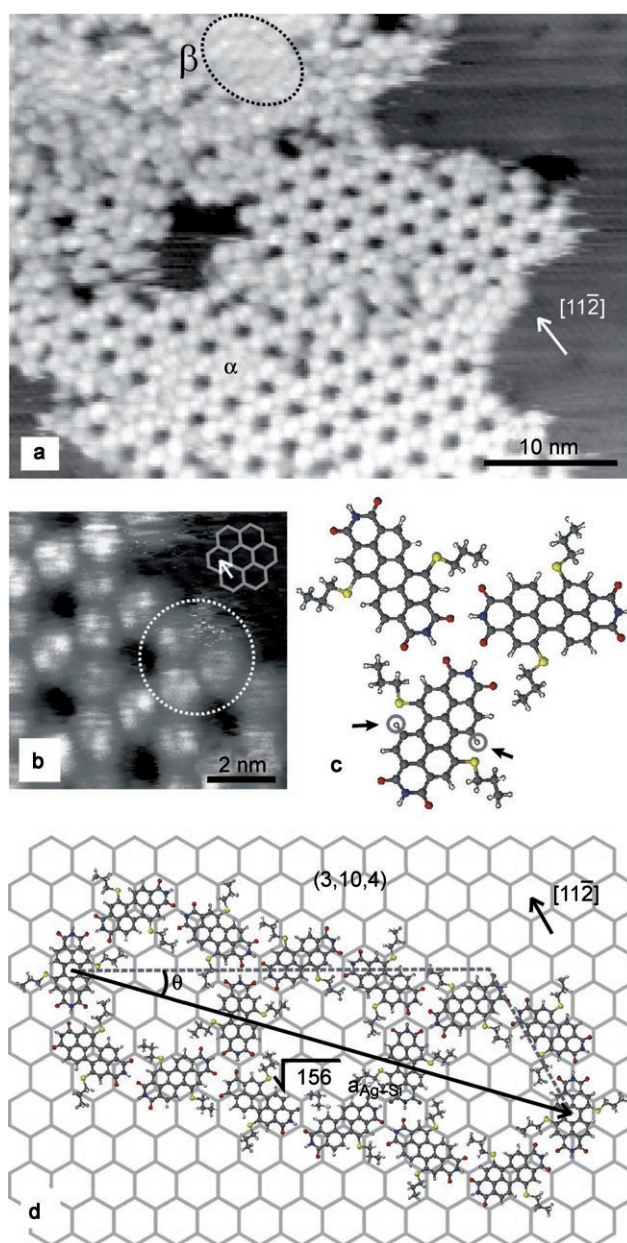


Figure 3. STM image ($V_{\text{sample}} = -2.5$ V, $I_{\text{tunnel}} = 0.03$ nA) after sublimation of di(propylthio)-PTCDI onto a Ag-Si(111) $\sqrt{3} \times \sqrt{3}R30^\circ$ surface. Two distinct domains were labelled with α for the hexagonal and β for the close-packed arrangement. b) Magnified image ($V_{\text{sample}} = -2.5$ V, $I_{\text{tunnel}} = 0.03$ nA) of a hexagonal region (α), in which a trimer node is highlighted with a dashed white circle and the surface reconstruction represented with a hexagonal mesh. c) Molecular model proposed for the trimer vertex highlighted in the previous image. The hydrogen atoms highlighted with grey circles and with arrows are alternative attachment sites for the propylthio chains as discussed in text. d) Schematic model proposed for the (10,4,3) molecular registry with the substrate. The arrow represents the periodicity of the arrangement of $\sqrt{156}a_{\text{Ag-Si}}$ (three hexagonal spacings of the molecular network), and the dashed lines detail each to the $10a_{\text{Ag-Si}}$ and $4a_{\text{Ag-Si}}$ periods of the surface. θ is defined as the angle between the pore-pore direction of the molecular network and one of the $\langle 11\bar{2} \rangle$ directions of the reconstructed Ag-Si(111) $\sqrt{3} \times \sqrt{3}R30^\circ$ surface. The arrangement is composed with trimers identical to that shown in part c), but with opposite chirality for information. The dimension of each STM image is given in the inserted scale bar.

The hexagonal arrangement is composed of an array of these trigonal vertices as shown schematically in Figure 3d. Based on the measured angles and periodicity of the arrangement, we propose a model that is commensurate with the substrate, with indices (l,m,n) (notation used in references [27a–c]) for hexagonal molecular arrangements on hexagonally reconstructed surfaces of (3,10,4), and a periodicity of $\sqrt{156}a_{\text{Ag-Si}} = 82.9 \text{ \AA}$ (see Figure 3d), corresponding to a pore-to-pore distance of 27.6 \AA . According to this model the pore-to-pore direction forms an angle of $\pm 16.1^\circ$ with the substrate $\langle 11\bar{2} \rangle$ direction. These values are in good agreement with those observed experimentally.

There are two possible angles (positive or negative) that this molecular arrangement may adopt relative to the substrate while observing the commensurability indicated with the indices above. In the trimer configuration given in Figure 3d (positive angle), the direction of the end-to-end axis of the molecules is parallel to the $\langle 1\bar{1}0 \rangle$ direction, whereas the negative angle and opposite chirality (Figure 3c) leads to molecules being parallel to the $\langle 11\bar{2} \rangle$ substrate direction. Our STM images reveal that we only observe one molecular orientation relative to the substrate which corresponds to the long axis of the molecule (intersecting the imide groups) parallel to the $\langle 1\bar{1}0 \rangle$ direction, as represented in Figure 3d. We also note that in the proposed model the molecules are all centred above high-symmetry positions (either Si or Ag trimers) in the reconstructed surface. This structure offers an alternative route to the formation of hexagonal porous networks, such as PTCDI/melamine and Br_2 -PTCDI/melamine, but with a smaller pore size and using a single molecule species.

Figure 4a shows STM images obtained after deposition of melamine on the sample discussed above (deposition time $\approx 4 \text{ h}$ with sample held at $60\text{--}80^\circ\text{C}$). These images show the formation of hexagonal networks with periodicity and orientation relative to the substrate that is identical to the PTCDI/melamine and Br_2 -PTCDI/melamine bimolecular structures (Figure 4b). This indicates that the unimolecular di(propylthio)-PTCDI hexagonal array has been converted into a bimolecular di(propylthio)-PTCDI/melamine hexagonal phase. The changes in network dimension through addition of melamine demonstrate an interesting, and we believe first demonstration of, sequential development of self-assembled structures with increasing porosity.

Deposition of C_{60} onto the hexagonal network, Figure 4c gives rise to a very different entrapment behaviour relative to the Br_2 -PTCDI/melamine and PTCDI/melamine networks;^[16] we see no evidence for heptamers or hexamers within the pores. It is possible to identify some fullerenes over some of the constituent molecules of the network as well as within the pores, but in an irregular fashion. A close inspection of the images shows that the underlying hexagonal structure is preserved demonstrating that the presence of the propylthio chains in the cavities inhibits the entrapment of fullerene molecules. This is most likely due to a steric hindering effect of the C_{60} -surface interaction as a

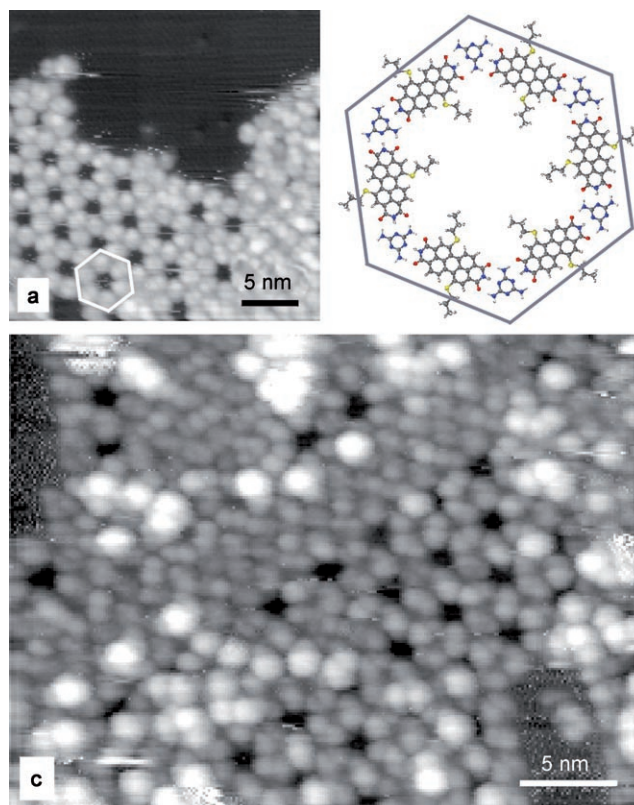


Figure 4. a) STM image ($V_{\text{sample}} = -2.5 \text{ V}$, $I_{\text{tunnel}} = 0.03 \text{ nA}$) showing the bimolecular hexagonal network formed after sublimation of melamine onto adsorbed di(propylthio)-PTCDI. b) Molecular model of the arrangement highlighted in (a). c) STM image ($V_{\text{sample}} = -2.3 \text{ V}$, $I_{\text{tunnel}} = 0.03 \text{ nA}$) after deposition of C_{60} onto the bimolecular honeycomb network. The dimension of each STM image is given in the inserted scale bar.

result of the presence of the propylthio chains providing a partial coverage of alkane chains within the pore.

Conclusion

We have demonstrated that the self-assembly and entrapment properties of surface-based supramolecular arrays may be controlled through the addition of simple functional groups to molecular building blocks. The incorporation of bromine in the bay region of PTCDI leads to a reduction in inter-row coupling and a preference for one-dimensional growth, as opposed to the formation of close-packed two-dimensional islands. The self-assembly of a unimolecular hexagonal arrangement in di(propylthio)-PTCDI is particularly noteworthy, illustrating the stabilising effect on introducing short-chain side groups to the PTCDI scaffold. Moreover we have demonstrated that the chemical functionalisation of the bay region of PTCDI provides a route for the rational introduction of chemically active groups on the perimeter of the pores formed in a two-dimensional supramolecular network. The modification of the unimolecular di(propylthio)-PTCDI hexagonal array to the bimolecular di(propylthio)-PTCDI/melamine array, resulting in a stepwise increase in

network periodicity, represents an example of dimensional control of porous-surface-based self-assembled structures through the exploitation of an additional supramolecular synthon. The contrasting entrapment behaviour observed with the di(propylthio)-PTCDI/melamine hexagonal networks relative to PTCDI/melamine and Br₂-PTCDI/melamine systems demonstrates the potential for control, through selection of side chains, of the properties of these cavities. Since Br₂-PTCDI is the precursor to many other functionalised R₂-PTCDI derivatives, with potentially more reactive attached groups, our work represents important progress towards the objective of combining chemically selectivity with spatial organisation within two dimensional nanoporous networks.

Experimental Section

Perylene-3,4:9,10-tetracarboxylic acid (Aldrich) was brominated according to a literature procedure^[26] and converted to *N,N'*-bis(*n*-butyl)-dibromo-3,4:9,10-perylenetetracarboxylic diimide with *n*-butylamine in butanol/H₂O.^[26] All reactions were carried out under an atmosphere of nitrogen. Column chromatography was performed on silica gel (Merck silica gel 60, 0.2–0.5 mm, 50–130 mesh). The ¹H NMR (300 MHz) and ¹³C NMR (75 MHz) spectra were obtained on a Bruker DPX 300 spectrometer. Microanalyses were performed by Stephen Boyer, London Metropolitan University. MS spectra (MALDI-TOF-MS) were determined on a Voyager-DE-STR mass spectrometer.

***N,N'*-Di(*n*-butyl)dipropylthioperylene-3,4:9,10-tetracarboxylic acid diimide (mixture of 1,7- and 1,6-isomers) (1):** *N,N'*-Di(*n*-butyl)-1,7-dibromoperylene-3,4:9,10-tetracarboxylic acid diimide^[26] (660 mg, 1 mmol), NaOH (100 mg, 2.5 mmol) and propanethiol (0.19 mL, 3 mmol) were suspended in pyridine (30 mL) and heated under reflux for 3 h. The progress of the reaction was followed by thin-layer chromatography with CH₂Cl₂ as eluent. After cooling to room temperature, the mixture was poured into 10% HCl and extracted with CH₂Cl₂. The organic phase was dried over Na₂SO₄, filtered and concentrated. The crude product was pure enough at this stage for further reaction procedures. For samples for analysis, the compound can be purified by column chromatography (silica) with CH₂Cl₂/hexane (5:1) as eluent allowing partial separation of the isomers. Yield 93%; ¹H NMR (CDCl₃): δ = 8.78 (d, *J* = 8 Hz, 2H), 8.73 (s, 2H), 8.65 (d, *J* = 8 Hz, 2H), 4.24 (t, *J* = 7 Hz, 4H; NCH₂), 3.20 (t, *J* = 7 Hz, 4H; SCH₂), 1.73 (m, 8H), 1.46 (m, 4H), 1.05 ppm (m, 12H; CH₃); ¹³C NMR (CDCl₃): δ = 163.86, 163.75, 138.86, 133.03, 132.87, 131.23, 129.30, 129.25, 128.75, 125.69, 122.37, 121.89, 40.86, 38.30, 31.33, 30.64, 22.38, 20.82, 14.26, 13.99 ppm; MS (MALDI-TOF): *m/z*: 650.6 [*M*⁺].

Dipropylthioperylene-3,4:9,10-tetracarboxydianhydride (mixture of 1,7- and 1,6-isomers) (2): Compound 1 (650 mg, 1 mmol; mixture of isomers) was dissolved in *i*PrOH (20 mL) and finely ground KOH (5.7 g, 100 mmol) was added. The suspension was sonicated for 15 min and subsequently heated under reflux for 4 h. The progress of the reaction was followed by thin-layer chromatography with CH₂Cl₂ as eluent. After cooling to room temperature the mixture was poured into 50% acetic acid and stirred for 1 h. The precipitate was filtered, redissolved in CH₂Cl₂ and washed with water. The organic phase was dried over Na₂SO₄, filtered and concentrated to yield a red powder (525 mg, 95% yield). ¹H NMR (CDCl₃): δ = 8.93 (d, *J* = 8 Hz, 2H), 8.88 (s, 2H), 8.74 (d, *J* = 8 Hz, 2H), 3.23 (t, *J* = 7 Hz, 4H; SCH₂), 1.72 (m, 4H), 1.05 ppm (m, 6H; CH₃); ¹³C NMR (CDCl₃): δ = 160.43, 159.97, 140.62, 134.03, 133.52, 132.96, 131.39, 129.88, 129.37, 127.92, 118.76, 118.45, 38.37, 22.25, 13.91 ppm; MS (MALDI-TOF): *m/z*: 540.3 [*M*⁺].

***N,N'*-Di[(2,4-dimethoxy)benzyl]dipropylthioperylene-3,4:9,10-tetracarboxylic acid diimide (mixture of 1,7- and 1,6-isomers) (4):** An identical

procedure was used as for the synthesis of 1, but with *N,N'*-di[(2,4-dimethoxy)benzyl]-1,7-dibromoperylene-3,4:9,10-tetracarboxylic acid diimide as a starting material. ¹H NMR (CDCl₃): δ = 8.87 (d, *J* = 8 Hz, 2H), 8.81 (s, 2H), 8.73 (d, *J* = 8 Hz, 2H), 7.12 (d, *J* = 9 Hz, 2H), 6.50 (s, 2H), 6.39 (d, *J* = 9 Hz, 2H), 5.43 (s, 2H), 3.90, 3.43 (2s, 6H each), 3.20 (t, *J* = 7 Hz, 4H; SCH₂), 1.72 (m, 4H), 1.05 ppm (m, 6H; CH₃); ¹³C NMR (CDCl₃): δ = 163.84, 163.77, 160.47, 158.61, 140.31, 138.96, 133.14, 132.95, 131.42, 129.45, 129.34, 128.86, 128.69, 125.84, 122.46, 121.99, 117.77, 104.52, 99.02, 56.02, 55.75, 39.242, 38.43, 22.38, 13.95 ppm; MS (MALDI-TOF): *m/z*: 838.8 [*M*⁺].

1,7-Dipropylsulfaneperylene-3,4:9,10-tetracarboxydiimide (mixture of 1,7- and 1,6-isomers) (3)

Synthesis from compound 2: Compound 2 (mixture of isomers; 160 mg, 0.3 mmol) was suspended in NH₄OH (20 mL) and heated under reflux overnight. The reaction mixture was cooled to room temperature and poured into glacial acetic acid in ice. The precipitate was filtered by gravity and dried in an oven overnight to yield a blue powder (75 mg, 47%), which exhibited very low solubility in common organic solvents.

Synthesis from compound 4: Compound 4 (250 mg, 0.3 mmol) was dissolved in toluene (20 mL), and methanesulfonic acid (2 mL) was added. The reaction mixture was heated under reflux for 4 h, over which time all perylene-containing material precipitated leaving a clear solution. The solvent was removed and the residue titrated with water, filtered and dried to yield 3 as a blue powder. Yield 89%; ¹H NMR (CDCl₃ + trifluoroacetic acid): δ = 9.08 (d, *J* = 8 Hz, 2H), 8.88 (s, 2H), 8.81 (d, *J* = 8 Hz, 2H), 3.27 (t, *J* = 7 Hz, 4H; SCH₂), 1.79 (m, 4H), 1.05 ppm (m, 6H; CH₃); MS (MALDI-TOF): *m/z*: 538.0 [*M*⁺].

Surface studies: The R₂-PTCDI and melamine deposition were performed under ultra-high vacuum (UHV) conditions (base pressure < 10⁻¹⁰ Torr). The Ag-Si(111)√3 × √3R30° surface (Ag-Si hereafter) was prepared under UHV by outgassing a 3 mm × 7 mm piece of a Si(111) substrate for > 12 h at 600–700 °C followed by flash annealing at 1150–1200 °C for approximately 60 s. This procedure results in the formation of a Si(111)-7 × 7 surface, which was converted to the Ag-Si by sublimation of Ag with the sample held at 500 °C.^[27] The evaporation rates for each R₂-PTCDI were measured with a quartz crystal microbalance and, for deposition of submonolayer coverages, crucible temperatures of 408 °C for Br₂-PTCDI and 340 °C for di(propylthio)-PTCDI were used. During R₂-PTCDI deposition, the sample was held at room temperature. Melamine was evaporated from a cell placed in a separate chamber to avoid cross-contamination. Images of the surface were acquired using a scanning tunneling microscope (STM) operating in constant current mode at room temperature. Electrochemically etched tungsten tips, cleaned prior to use by electron beam heating, were used throughout.

Density functional calculations: Density functional calculations were performed using established methodologies^[28] within the DMol³ package. See Supporting Information for more details.

Acknowledgements

This work was supported by the UK Engineering and Physical Sciences Research Council (EPSRC) under Grants Nos. GR/S97521/01 and EP/D048761/1 and the European Union Framework 6 Grant “NANO-MESH” (NMP4-CT-2004-013817). G.N.F. is grateful for the financial support from CAPES (Brazil).

- [1] K. Ariga, T. Kunitake, *Supramolecular Chemistry—Fundamentals and Applications*, Springer, Berlin, 2006.
- [2] J. V. Barth, G. Costantini, K. Kern, *Nature* 2005, 437, 671–679.
- [3] G. M. Whitesides, B. Grzybowski, *Science* 2002, 295, 2418–2421.
- [4] a) S. Hasegawa, S. Horike, R. Matsuda, S. Furukawa, K. Mochizuki, Y. Kinoshita, S. Kitagawa, *J. Am. Chem. Soc.* 2007, 129, 2607–2614; b) O. Crespo-Biel, C. W. Lim, B. J. Ravoo, D. N. Reinhoudt, J. Huskens, *J. Am. Chem. Soc.* 2006, 128, 17024–17032; c) V. A. Azov, A.

- Beeby, M. Cacciarini, A. G. Cheetham, F. Diederich, M. Frei, J. K. Gimzewski, V. Gramlich, B. Hecht, B. Jaun, T. Latychevskaia, A. Lieb, Y. Lill, F. Marotti, A. Schlegel, R. R. Schlittler, P. J. Skinner, P. Seiler, Y. Yamakoshi, *Adv. Funct. Mater.* **2006**, *16*, 147–156; d) M. Pittelkow, C. B. Nielsen, A. C. Broeren, J. L. J. van Dongen, M. H. P. van Genderen, E. W. Meijer, J. B. Christensen, *Chem. Eur. J.* **2005**, *11*, 5126–5135; e) C. A. Nijhuis, K. A. Dolatowska, B. J. Ravoo, J. Huskens, D. N. Reinhoudt, *Chem. Eur. J.* **2007**, *13*, 69–80; f) T. K. Maji, R. Matsuda, S. Kitagawa, *Nat. Mater.* **2007**, *6*, 142–148; g) M. P. Schramm, R. J. Hooley, J. Rebek, *J. Am. Chem. Soc.* **2007**, *129*, 9773–9779.
- [5] T. Yokoyama, S. Yokoyama, T. Kamikado, Y. Okuno, S. Mashiko, *Nature* **2001**, *413*, 619–621.
- [6] J. V. Barth, J. Weckesser, C. Cai, P. Günter, L. Bürgi, O. Jeandupeaux, K. Kern, *Angew. Chem.* **2000**, *112*, 1285–1288; *Angew. Chem. Int. Ed.* **2000**, *39*, 1230–1234.
- [7] H. Spillmann, A. Dmitriev, N. Lin, P. Messina, J. V. Barth, K. Kern, *J. Am. Chem. Soc.* **2003**, *125*, 10725–10728.
- [8] S. De Feyter, F. C. De Schryver, *Chem. Soc. Rev.* **2003**, *32*, 139–150.
- [9] S. Griessl, M. Lackinger, M. Edelwirth, M. Hietschold, W. M. Heckl, *Single Mol.* **2002**, *3*, 25–31; M. Blunt, X. Lin, M. C. Gimenez-Lopez, M. Schröder, N. R. Champness, P. H. Beton, *Chem. Commun.* **2008**, 2304–2306.
- [10] J. Lu, S.-B. Lei, Q.-D. Zeng, S.-Z. Kang, C. Wang, L.-J. Wan, C. Bai, *J. Phys. Chem. B* **2004**, *108*, 5161–5165.
- [11] R. Otero, M. Schöck, L. M. Molina, E. Lægsgaard, I. Stensgaard, B. Hammer, F. Besenbacher, *Angew. Chem.* **2005**, *117*, 2310–2315; *Angew. Chem. Int. Ed.* **2005**, *44*, 2270–2275.
- [12] C. Safarowsky, A. Rang, C. A. Schalley, K. Wandelt, P. Broekmann, *Electrochim. Acta* **2005**, *50*, 4257–4268.
- [13] M. Stöhr, M. Wahl, C. H. Galka, T. Riehm, T. A. Jung, L. H. Gade, *Angew. Chem.* **2005**, *117*, 7560–7564; *Angew. Chem. Int. Ed.* **2005**, *44*, 7394–7398.
- [14] G. Pawin, K. L. Wong, K.-Y. Kwon, L. A. Bartels, *Science* **2006**, *313*, 961–962.
- [15] J. A. Theobald, N. S. Oxtoby, M. A. Phillips, N. R. Champness, P. H. Beton, *Nature* **2003**, *424*, 1029–1031.
- [16] L. M. A. Perdigão, E. W. Perkins, J. Ma, P. A. Staniec, B. L. Rogers, N. R. Champness, P. H. Beton, *J. Phys. Chem. B* **2006**, *110*, 12539–12542.
- [17] P. A. Staniec, L. M. A. Perdigão, A. Saywell, N. R. Champness, P. H. Beton, *ChemPhysChem* **2007**, *8*, 2177–2181.
- [18] B. Xu, C. Tao, W. G. Cullen, J. E. Reutt-Robey, E. D. Williams, *Nano Lett.* **2005**, *5*, 2207–2211.
- [19] H. Spillmann, A. Kiebele, M. Stöhr, T. A. Jung, O. Bonifazi, F. Cheng, F. Diederich, *Adv. Mater.* **2006**, *18*, 275–279.
- [20] a) S. Stepanow, M. Lingenfelder, A. Dmitriev, H. Spillmann, E. Delvigne, N. Lin, X. Deng, C. Cai, J. V. Barth, K. Kern, *Nat. Mater.* **2004**, *3*, 229–233; b) S. Stepanow, N. Lin, D. Payer, U. Schlickum, F. Klappenberger, G. Zoppellaro, M. Ruben, H. Brune, J. V. Barth, K. Kern, *Angew. Chem.* **2007**, *119*, 724–727; *Angew. Chem. Int. Ed.* **2007**, *46*, 710–713. M. Ruben, D. Payer, A. Landa, A. Comisso, C. Gattinoni, N. Lin, J.-P. Collin, J.-P. Sauvage, A. De Vita, K. Kern, *J. Am. Chem. Soc.* **2006**, *128*, 15644–15651.
- [21] M. Böhlinger, K. Morgenstern, W. D. Schneider, R. Berndt, *Angew. Chem.* **1999**, *111*, 832; *Angew. Chem. Int. Ed.* **1999**, *38*, 821.
- [22] H. L. Zhang, W. Chen, L. Chen, H. Huang, X. S. Wang, J. Yuhara, A. T. S. Wee, *Small* **2007**, *3*, 2015–2018.
- [23] Q. Chen, D. J. Frankel, N. V. Richardson *Langmuir* **2002**, *18*, 3219.
- [24] a) F. Würthner, *Chem. Commun.* **2004**, 1564; b) H. Langhals, *Heterocycles* **1995**, *40*, 477; c) B. Yoo, T. Jung, D. Basu, A. Dodabalapur, B. A. Jones, A. Faccetti, M. R. Wasielewski, T. J. Marks, *Appl. Phys. Lett.* **2006**, *88*, 082104; d) K.-Y. Law, *Chem. Rev.* **1993**, *93*, 449; e) G. Horowitz, F. Kouki, P. Spearman, D. Fichou, C. Nogeus, X. Pan, F. Garnier, *Adv. Mater.* **1996**, *8*, 224; f) C. W. Tang, *Appl. Phys. Lett.* **1986**, *48*, 183; g) J. Q. Ou, C. Kohl, M. Pottel, K. Mullen, *Angew. Chem.* **2004**, *116*, 1554; *Angew. Chem. Int. Ed.* **2004**, *43*, 1528; h) F. Würthner, C. Thalacker, S. Diele, C. Tschierske, *Chem. Eur. J.* **2001**, *7*, 2245.
- [25] a) T. E. Kaiser, H. Wang, V. Stepanenko, F. Würthner, *Angew. Chem.* **2007**, *119*, 5637–5640; *Angew. Chem. Int. Ed.* **2007**, *46*, 5541–5544; b) E. H. A. Beckers, Z. Chen, S. C. J. Meskers, P. Jonkheijm, A. P. H. J. Schenning, X.-Q. Li, P. Osswald, F. Würthner, R. A. J. Janssen, *J. Phys. Chem. B* **2006**, *110*, 16967–16978; c) Y. Liu, J. Zhuang, H. Liu, Y. Li, F. Lu, H. Gan, T. Jiu, N. Wang, X. He, D. Zhu, *ChemPhysChem* **2004**, *5*, 1210–1215; d) F. Würthner, Z. Chen, F. J. M. Hoeben, P. Osswald, C.-C. You, P. Jonkheijm, J. von Herrikhuyzen, A. P. H. J. Schenning, P. P. A. M. van der Schoot, E. W. Meijer, E. H. A. Beckers, S. C. J. Meskers, R. A. J. Janssen, *J. Am. Chem. Soc.* **2004**, *126*, 10611–10618; e) Y. Liu, S. Xiao, H. Li, Y. Li, H. Liu, F. Lu, J. Zhuang, D. Zhu, *J. Phys. Chem. B* **2004**, *108*, 6256–6260; f) A. P. H. J. Schenning, J. van Herrikhuyzen, P. Jonkheijm, Z. Chen, F. Würthner, E. W. Meijer, *J. Am. Chem. Soc.* **2002**, *124*, 10252–10253; g) F. Würthner, C. Thalacker, A. Sautter, W. Schartl, W. Ibach, O. Hollricher, *Chem. Eur. J.* **2000**, *6*, 3871–3886; h) F. Würthner, C. Thalacker, A. Sautter, *Adv. Mater.* **1999**, *11*, 754–758.
- [26] a) C.-C. Chao, M.-K. Leung, Y. O. Su, K.-Y. Chiu, T.-H. Lin, S.-J. Shieh, S.-C. Lin, *J. Org. Chem.* **2005**, *70*, 4323–4331; b) F. Würthner, V. Stepanenko, Z. Chen, C. R. Saha-Möller, N. Kocher, D. Stalke, *J. Org. Chem.* **2004**, *69*, 7933–7939.
- [27] a) M. D. Upward, P. Moriarty, P. H. Beton, *Phys. Rev. B* **1997**, *56*, R1704–R1707; b) M. J. Butcher, J. W. Nolan, M. R. C. Hunt, P. H. Beton, L. Dunsch, P. Kuran, P. Georgi, T. J. S. Dennis, *Phys. Rev. B* **2001**, *64*, 195401; c) M. D. Upward, P. H. Beton, P. Moriarty, *P. Surf. Sci.* **1999**, *441*, 21–25; d) T. Takahashi, S. Nakatani, N. Okamoto, T. Ichikawa, S. Kikuta, *Surf. Sci.* **1991**, *242*, 54–58; e) M. Katayama, R. S. Williams, M. Kato, E. Nomura, M. Aono, *Phys. Rev. Lett.* **1991**, *66*, 2762–2765.
- [28] J. C. Swarbrick, J. Ma, J. A. Theobald, N. S. Oxtoby, J. N. O'Shea, N. R. Champness, P. H. Beton, *J. Phys. Chem. B* **2005**, *109*, 12167–12174.
- [29] M. E. Cañas-Ventura, W. Xiao, D. Wasserfallen, K. Müllen, H. Brune, J. V. Barth, R. Fasel, *Angew. Chem.* **2007**, *119*, 1846–1850; *Angew. Chem. Int. Ed.* **2007**, *46*, 1814–1818.
- [30] M. Ruiz-Oses, N. Gonzalez-Lakunza, I. Silanes, A. Gourdon, A. Arnau, J. E. Ortega, *J. Phys. Chem. B* **2006**, *110*, 25573–25577.
- [31] D. L. Keeling, N. S. Oxtoby, C. Wilson, M. J. Humphry, N. R. Champness, P. H. Beton, *Nano Lett.* **2003**, *3*, 9–12.
- [32] J. B. Taylor, P. H. Beton, *Phys. Rev. Lett.* **2006**, *97*, 236102.
- [33] U. K. Weber, V. M. Burlakov, L. M. A. Perdigão, R. H. J. Fawcett, P. H. Beton, N. R. Champness, J. H. Jefferson, G. A. D. Briggs, D. G. Pettifor, *Phys. Rev. Lett.* **2008**, *100*, 156101.
- [34] a) L. M. A. Perdigão, N. R. Champness, P. H. Beton, *Chem. Commun.* **2006**, 538–540; b) P. A. Staniec, L. M. A. Perdigão, B. L. Rogers, N. R. Champness, P. H. Beton, *J. Phys. Chem. C* **2007**, *111*, 886–893.
- [35] F. Klappenberger, M. E. Canas-Ventura, S. Clair, S. Pons, U. Schlickum, Z. R. Qu, H. Brune, K. Kern, T. Strunskus, C. Wöll, A. Comis- sa, A. de Vita, M. Ruben, J. V. Barth, *ChemPhysChem* **2007**, *8*, 1782–1786.
- [36] a) B. Delley, *J. Chem. Phys.* **1990**, *92*, 508–517; b) B. Delley, *J. Chem. Phys.* **2000**, *113*, 7756–7764; c) J. P. Perdew, K. Burke, M. Ernzerhof, *Phys. Rev. Lett.* **1996**, *77*, 3865–3868.

Received: March 14, 2008
Published online: July 30, 2008